Report LR-666

The Compressive Properties of GLARE

November 1991

J.L. Verolme

TU Delft

Faculty of Aerospace Engineering

Delft University of Technology

Report LR-666

The Compressive Properties of GLARE

November 1991

J.L. Verolme

Table of contents

Summary

GLARE® is a member of a family of hybrid materials called ARALL®. ARALL is a composite material consisting of alternating thin aluminium alloy sheets and unidirectional or cross-ply layers of preimpregnated fibers (so-called prepreg). In GLARE, the prepreg consists of high strength glass fibers (R and S_2) and epoxy resin and the aluminium alloy used is either 2024-T3, 7075-T6 or 7475-T6.

Among the basic mechanical properties needed for the certification of a new (aircraft) material are the compressive properties. Since the compressive properties of GLARE -a relatively new material- as yet were unknown (June 1990), a complete investigation is carried out: from GLARE 1 to GLARE 4 several lay-ups* were tested in longitudinal as well as in longitudinal-transverse direction.

To check whether Young's modulus and the yield stress can be predicted accurately theoretically, prediction methods based on simple formulas are developed. For this purpose pure aluminium alloy and pure prepreg specimens were tested. It is shown that simple methods already lead to accurate (90 % and more) predictions.

To investigate the effect of the post-stretch percentage on the yield stress of GLARE 1, as-cured material is also examined. As expected, the compressive yield stress lowers with increasing post-stretch percentage.

To show the abilities of GLARE in compression, structural efficiency curves were created.

*A X/(X-1) lay-up consists of X layers of aluminium and consequently (X-1) layers of prepreg.

List of symbols

A	area
b	width
C_1 & C_2	constants depending on stringer-skin panel dimensions
D_{ij}	bending stiffness of a laminate
E	Young's modulus
G	shear modulus
I	moment of inertia
L	length
p	panel loading (in N/mm)
t	thickness
$\bar{t}$	equivalent thickness
W	weight
α	coefficient of thermal expansion
β	efficiency parameter
ΔT	$= T_{use} - T_{cure} = -100\ ^{0}C$
ϵ	strain
$\epsilon_{1,pl}$	post-stretch percentage
Σ	summation (e.g. Σt = sum of all layers)
σ	stress
σ^2	standard deviation of the test results
ρ	density
μ	Poisson's ratio

Indices

al	aluminium
c	compression
e	effective
exp	experimental
f	flexural
l	local
o	initial
pr	prepreg
theor	theoretical
T	temperature
ult	ultimate
x,y	laminate coordinates
1,2	principle material coordinates or (internal stresses in) respectively prepreg and aluminium layers
0.2	offset of 0.2 %

Sign convention

Compressive stresses and strains are negative, and tensile stresses and strains are positive. In tables and figures, however, if the subscription mentions compression, no minus sign is used. This was also used in the paragraph concerning structural efficiency plots.

Chapter 1 : Introduction

ARALL® is a family of hybrid materials, developed by the Faculty of Aerospace Engineering of Delft University of Technology. These materials are bonded arrangements of thin aluminium alloy sheets and alternating plies of epoxy adhesive impregnated with either unidirectional or cross-ply fibers. A cross-section of ARALL laminate is shown in *Figure 1.1*. ARALL is developed to satisfy the need for a new aircraft material that combines high strength, low density and a high Young's modulus with improved toughness, corrosion resistance and fatigue properties. Especially the good fatigue and impact resistance of the material is striking. More details about ARALL can be found in *Literature 1.1* to *1.6*.
The material examined in this report consists of Ciba-Geigy Fibredux 925 prepreg (R-glass fibers impregnated with epoxy resin) and either the 7075-T6 or the 2024-T3 aluminium alloy. The trade name of this material is GLARE®. GLARE is commercially available in four grades. The general lay-out of these grades is listed in *Table 1.1*.

The compressive properties of GLARE -part of the important data needed for the certification of this new aircraft material- as yet were unknown (June 1990). The object of this inquiry is therefore to determine the compressive behaviour of the complete range of GLARE. Several lay-ups of all grades of GLARE were tested in longitudinal (L) and longitudinal-transverse (LT) direction.
In order to develop prediction methods for Young's modulus and yield stress, pure aluminium (also as a reference) and pure prepreg specimens were tested.

Grade	Aluminium-Alloy		Prepreg		Post-Stretched
	type	thickness (mm)	composition	orientation	
GLARE 1	7075-T6	0.3	glass/epoxy	U.D.	0.5 %
GLARE 2	2024-T3	0.3	glass/epoxy	U.D.	-
GLARE 3	2024-T3	0.3	glass/epoxy	cross-ply (50/50)	-
GLARE 4	2024-T3	0.3	glass/epoxy	cross-ply (70/30)	-

Table 1.1 : Grades of GLARE.

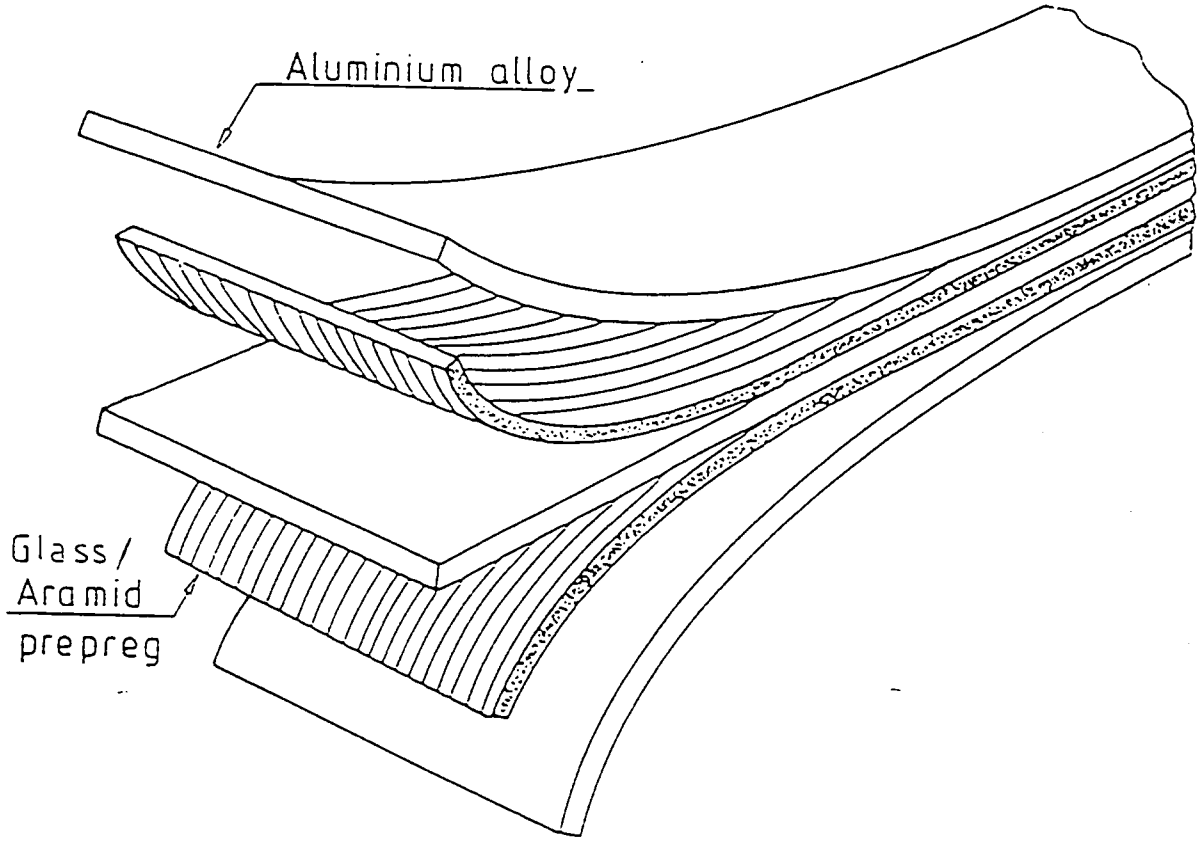

Figure 1.1 : ARALL/GLARE laminates;
schematic of standard 3/2 lay-up.

To show the effect of the post-stretch percentage on the yield stress of GLARE 1, as-cured GLARE 1 specimens were tested too.

The excellent behaviour in compression of GLARE with regard to aluminium and ARALL is shown also by structural efficiency curves.

In the second chapter the production of GLARE and the test specimen will be discussed. The third chapter shows and explains the test set-up. In chapter four the compressive properties are determined from the test results and the structural efficiency curves are deduced. In chapter five the above mentioned properties are predicted. Finally the predicted and experimental values are compared and some conclusions are drawn.

Chapter 2 : Specimen preparation

Before laminating the aluminium and the prepreg layers, a surface treatment must be applied to the aluminium. This is necessary for a good adhesion between the aluminium and the prepreg layers. The aluminium is given the following chemical treatment:

1 First it is degreased by P3RST, an alkaline product.

2 Afterwards the aluminium is pickled in chromic-sulphuric acid to remove the old film of oxide.

3 Anodizing in chromic acid follows to create a new thick film of oxide on the aluminium which provides long term adhesion.

4 Finally the aluminium is primed (BR127) to protect the new film of oxide and to assure good wetting.

After lay-up the material is cured in an autoclave. This curing process will, because of the thermal mismatch, result in tensile residual stress in the aluminium layers. This, especially for fatigue, unfavourable tensile stress can be changed into a compressive one by plastically deforming the material after curing. This is achieved by giving the material 0.5 % plastic deformation.

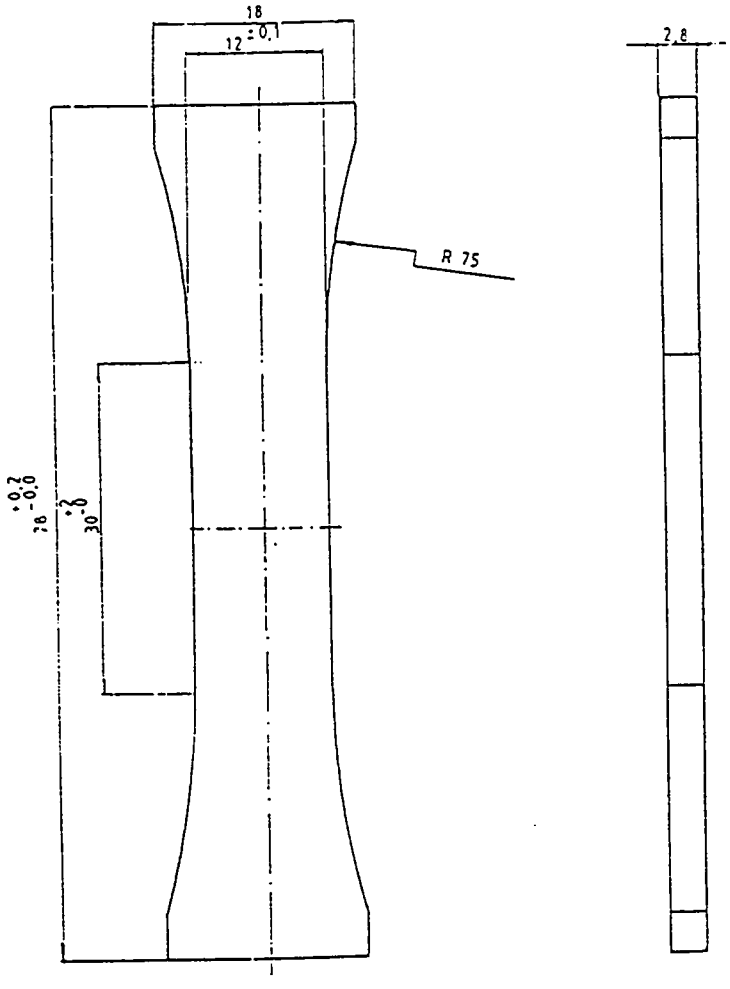

Figure 2.1 : Shape of the test specimen prescribed by DIN standard 53454.

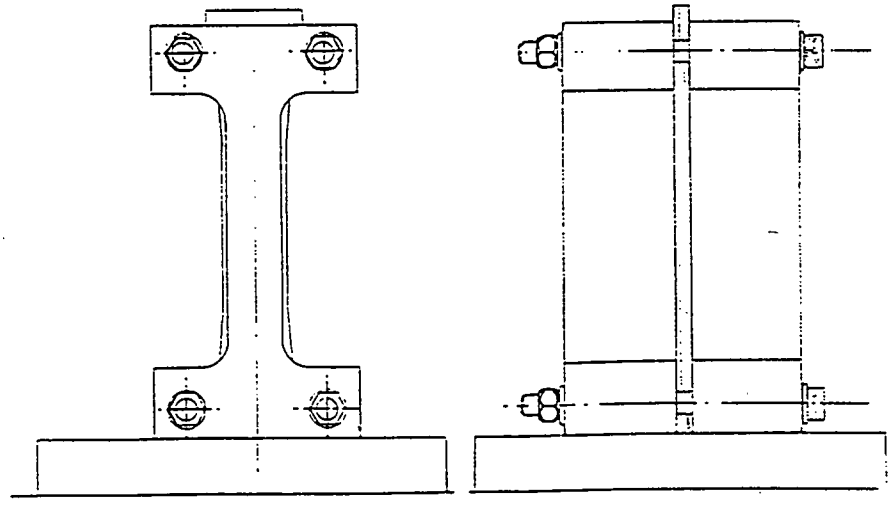

Figure 2.2 : Specimen with anti-buckling device in position.

The compressive tests are carried out according to DIN standard 53454. A small summary of relevant facts:

- The shape of the test specimen prescribed by the standard is shown in *Figure 2.1*.
- The use of an anti-buckling device is advised. The specimen with the anti-buckling device is shown in *Figure 2.2*.
- The standard mentions a loading rate of 0.035 mm/s.
- At least six specimens must be tested.

Several layers of GLARE were bonded together to prevent buckling of the part of the specimen which extends above the anti-buckling device. In practice this means bonding three layers of 2/1 lay-up and two layers of 3/2 and 4/3 lay-up, which have a nominal thickness of respectively 0.85, 1.4 and 1.95 mm.
The ultimate shape of the specimen is obtained by milling.

Chapter 3 : Test set-up

The tests are carried out on a 10-tons compression test machine. The machine is displacement controlled. A loading rate of 0.005 mm/s is used, instead of the normalized 0.035 mm/s (the engine controlling the load speed only has two possible positions, the slowest one is chosen to be able to control the test better). According to the standard the specimen is supported by an anti-buckling device. Between the device and the specimen a thin layer of teflon is used. The specimen and the teflon are slightly oiled to further reduce the drag.
An X-Y recorder is used to draw a load-displacement graph. The displacement is measured by a small extensometer. The offset distance between the knives of the extensometer is 10 mm.

Chapter 4 : Test evaluations

§ 4.1 : Young's modulus

Young's modulus in compression E_c is defined as the ratio between the compressive stress on a body and the shortening per unit length resulted by this force. This modulus can be deduced from the force-displacement graph.
The results for GLARE are listed in *Table 4.1*. The obtained as-cured GLARE 1 values are tabled in *Table 4.2* and the results for the aluminium alloy (bare) and the prepreg specimens are listed in *Table 4.3*.

grade	layup	thickness (mm)	direction	E_c (GPa)	σ^2 (st.dev.)
as-cured *GLARE 1*	2/1	0.89	L	66.8	0.79
			LT	54.0	0.33
as-cured *GLARE 1*	3/2	1.47	L	65.0	0.91
			LT	51.1	0.43
as-cured *GLARE 1*	4/3	2.05	L	62.8	0.59
			LT	47.7	0.45

Table 4.2 : Young's modulus in compression of as-cured GLARE 1 (six specimens).

grade	layup	thickness (mm)	direction	E_c (GPa)	σ^2 (st.dev.)
post-st. *GLARE 1*	2/1	0.84	L	67.7	1.68
			LT	56.2	0.65
post-st. *GLARE 1*	3/2	1.41	L	66.5	1.09
			LT	51.1	0.69
post-st. *GLARE 1*	4/3	2.04	L	62.4	1.16
			LT	47.3	0.47
GLARE 2	2/1	0.83	L	69.2	0.53
			LT	56.4	0.90
GLARE 2	3/2	1.34	L	68.3	0.81
			LT	53.2	0.61
GLARE 2	4/3	1.90	L	67.4	0.38
			LT	51.2	0.86
GLARE 3	2/1	0.82	L	62.8	0.37
			LT	61.8	0.35
GLARE 3	3/2	1.38	L	59.5	0.27
			LT	59.7	0.29
GLARE 4	2/1	0.95	L	62.0	0.35
			LT	56.5	0.82
GLARE 4	3/2	1.59	L	60.8	0.70
			LT	54.4	0.45

Remark: post-st. means post-stretched.

Table 4.1 : Young's modulus in compression of GLARE (six specimens).

type	thickness (mm)	direction	E_c (GPa)	σ^2 (st.dev.)
2024-T3	2.00	L	75.8	0.50
		LT	75.8	1.14
7075-T6	2.00	L	74.0	0.40
		LT	74.3	1.06
GLASS UD	2.00	L	53.1	0.73
		LT	11.2	0.66
GLASS-CROSS 50-50	2.00	L & LT	33.4	0.42
GLASS-CROSS 70-30	2.00	L	38.7	0.69
		LT	25.4	0.66

Table 4.3 : Young's modulus in compression for aluminium and R-glass prepreg (six specimens).

§ 4.2 : Yield stress

The compressive yield stress is defined as the stress at which after unloading 0.2% permanent deformation is given to the material.
The obtained values for GLARE are listed in *Table 4.4* and for aluminium listed in *Table 4.6*. In *Table 4.5* the values for as-cured GLARE 1 are given. Pure prepreg is behaving perfectly elastic until failure, so it has no yield stress.

grade	layup	thickness (mm)	direction	$\sigma_{0.2}$ (MPa)	σ^2 (st.dev.)
post-st. *GLARE 1*	2/1	0.84	L	446.5	9.78
			LT	427.0	6.14
post-st. *GLARE 1*	3/2	1.41	L	423.7	6.42
			LT	402.7	1.78
post-st. *GLARE 1*	4/3	2.04	L	406.5	10.92
			LT	374.5	3.90
GLARE 2	2/1	0.83	L	389.5	3.23
			LT	252.5	1.00
GLARE 2	3/2	1.34	L	420.0	9.32
			LT	241.0	1.61
GLARE 2	4/3	1.90	L	421.7	3.64
			LT	232.2	2.19
GLARE 3	2/1	0.82	L	319.3	3.13
			LT	318.2	6.00
GLARE 3	3/2	1.38	L	314.4	3.93
			LT	316.4	7.42
GLARE 4	2/1	0.95	L	349.0	5.92
			LT	299.2	6.10
GLARE 4	3/2	1.59	L	370.9	9.46
			LT	291.5	2.01

Remark: post-st. means post-stretched.

Table 4.4 : The compressive yield stress of GLARE (six specimens).

grade	layup	thickness (mm)	direction	$\sigma_{0.2}$ (MPa)	σ^2 (st.dev.)
as-cured *GLARE 1*	2/1	0.89	L	546.4	9.04
			LT	400.1	6.42
as-cured *GLARE 1*	3/2	1.47	L	564.9	7.80
			LT	375.6	3.89
as-cured *GLARE 1*	4/3	2.05	L	576.6	2.45
			LT	344.5	2.08

Table 4.5 : The compressive yield stress of as-cured GLARE 1 (six specimens).

type	thickness (mm)	direction	$\sigma_{0.2}$ (MPa)	σ^2 (st.dev.)
2024-T3	2.00	L	306.9	2.91
		LT	347.6	2.54
7075-T6	2.00	L	533.1	3.13
		LT	543.7	5.67

Table 4.6 : The compressive yield stress of aluminium (six specimens).

§ 4.3 : Ultimate stress

For some types of GLARE an attempt is made to determine the ultimate compressive stress. In order to be sure that failure instead of buckling of the upper part of the specimen occurred, another two of the obtained laminates (so six times 2/1 lay-up and four times 3/2 and 4/3 lay-up) were bonded. Still several specimens buckled. The obtained values for the ultimate stress in buckling are in *Table 4.7*. *Figure 4.1* shows a photograph of that phenomenon.

grade	layup	direction	failure stress and st.dev.(σ^2)
GLARE 1	3/2	L	σ_{ult}= 448.4 MPa (σ^2=1.06)
GLARE 1	4/3	L	σ_{ult}= 649.5 MPa (σ^2= 5.10)

Table 4.7 : Ultimate stresses in compression of some GLARE types (buckling of the upper part of the specimen).

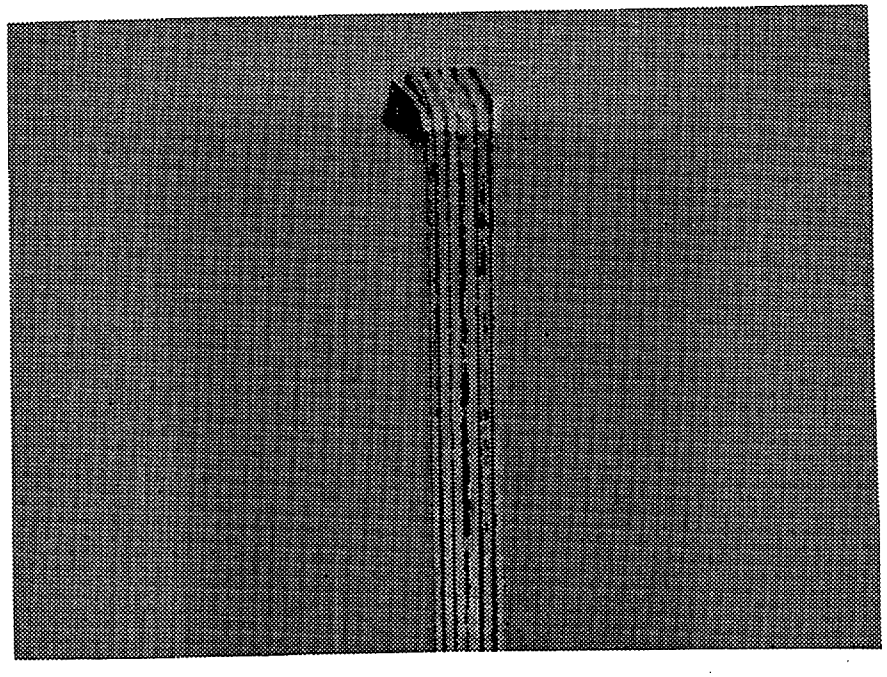

Figure 4.1 : Photograph of buckling of the upper part of the specimen.

The maximum compressive stress and the failure strain is given in *Table 4.8*. This failure mode is shown in *Figure 4.2*. It is obvious -from this photograph- that shear is the cause of failure.

grade	layup	direction	failure stress and st.dev.(σ^2)
GLARE 1	4/3	L	σ_{ult}= 805.5 MPa (*)
GLARE 2	3/2	L	σ_{ult}= 749.9 MPa (σ^2= 27.56)
GLARE 2	4/3	L	σ_{ult}= 755.1 MPa (σ^2= 65.6)
GLARE 3	2/1	L/LT	σ_{ult}= 554.0 MPa (σ^2= 6.16)
GLARE 3	3/2	L/LT	σ_{ult}= 549.6 MPa (σ^2= 19.62)

(*) Only one specimen showed failure

grade	layup	direction	maximum strain and st.dev.(σ^2)
GLARE 1	4/3	L	ϵ_{ult}= 3.2 % (*)
GLARE 2	3/2	L	ϵ_{ult}= 2.2 % (σ^2= 0.17)
GLARE 2	4/3	L	ϵ_{ult}= 2.36 % (σ^2= 0.07)
GLARE 3	2/1	L/LT	ϵ_{ult}= 2.7 % (σ^2= 0.07)
GLARE 3	3/2	L/LT	ϵ_{ult}= 2.5 % (σ^2= 0.23)

(*) Only one specimen showed failure

Table 4.8 : Ultimate stresses and strains in compression of some GLARE types (failure; "shear mode").

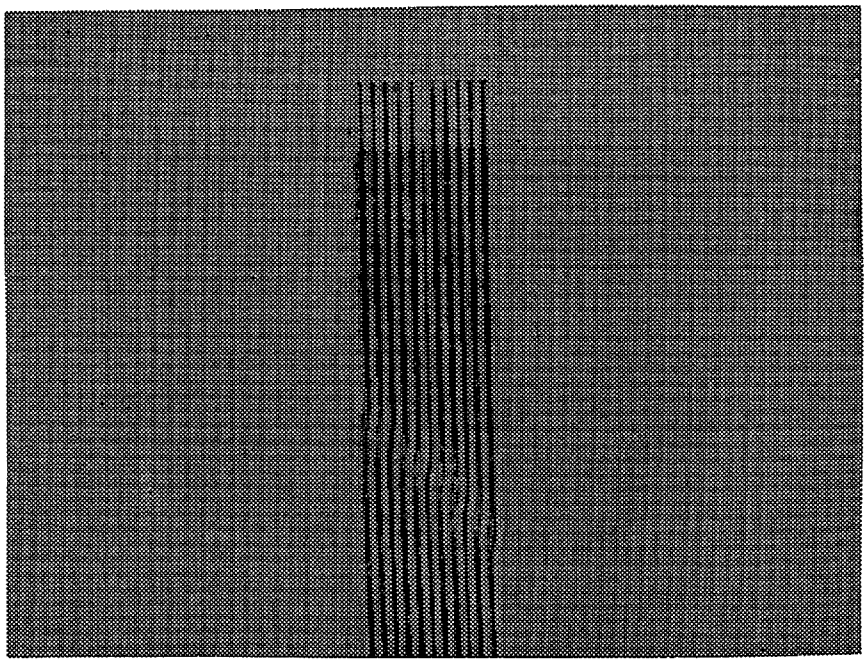

Figure 4.2 : Photograph of shear mode failure.

§ 4.4 : Structural efficiency plots

To compare materials for compressive critical components often so-called compression structural efficiency curves are created.

For a specific stringer-skin panel either the compressive weight index or the specific compressive strength is drawn as a function of the structural index.

The compressive weight index is defined as

$$\frac{W}{A.L_e}$$

with W = total weight of panel
A = area of panel
L_e = effective length of panel.

The factor σ/ρ is called the specific compressive strength (with ρ = density of the material).
The structural index p/L_e (with p = panel loading in N/mm) is a parameter for the loading intensity on the panel.
In this report the structural efficiency plots are created using the following demands:

1 No Euler buckling may occur.

2 The stress level does, in an aluminium panel, never exceed the yield stress. So, for aluminium the compressive yield stress is a cut-off value. In this report the same demand is used for GLARE and ARALL.

The two above mentioned demands can be formulated as a function of the structural index (more details can be found in the *appendix*):

1 **Panel buckling:**

$$\frac{\sigma}{\rho} = \frac{1}{\rho} \cdot \left(\frac{2\pi^2}{6} \right)^{1/4} \cdot \left(\frac{C_1}{C_2^2} \right)^{1/4} \cdot \beta^{1/4} \cdot \left(E_x . D^* \right)^{1/4} \cdot \sqrt{\frac{p}{L_e}}$$

and

$$\frac{W}{A.L_e} = \rho \cdot \left(\frac{6}{2\pi^2} \right)^{1/4} \cdot \left(\frac{C_2^2}{C_1} \right)^{1/4} \cdot \left(\frac{1}{\beta} \right)^{1/4} \cdot \left(\frac{1}{E_x . D^*} \right)^{1/4} \cdot \sqrt{\frac{p}{L_e}}$$

In these formulas

A = area of panel

$C_1 = \frac{\pi^2 . I}{b^2 . A}$

$C_2 = t/\bar{t}$

D^* = orthotropic local buckling coefficient

E_x = Young's modulus in x-direction

L_e = effective length of panel

p = panel loading

W = weight of panel

β = efficiency parameter

σ = stress level in panel.

ρ = density of material.

2 Yield stress cut-off value:

$$\frac{\sigma}{\rho} = \frac{\sigma_{0.2}}{\rho}$$

and

$$\frac{W}{A.L_e} = \frac{\rho}{\sigma_{0.2}} \cdot \frac{P}{L_e}$$

The structural efficiency curves can be found in *Figure 4.3* (strength) and *Figure 4.4* (weight index).

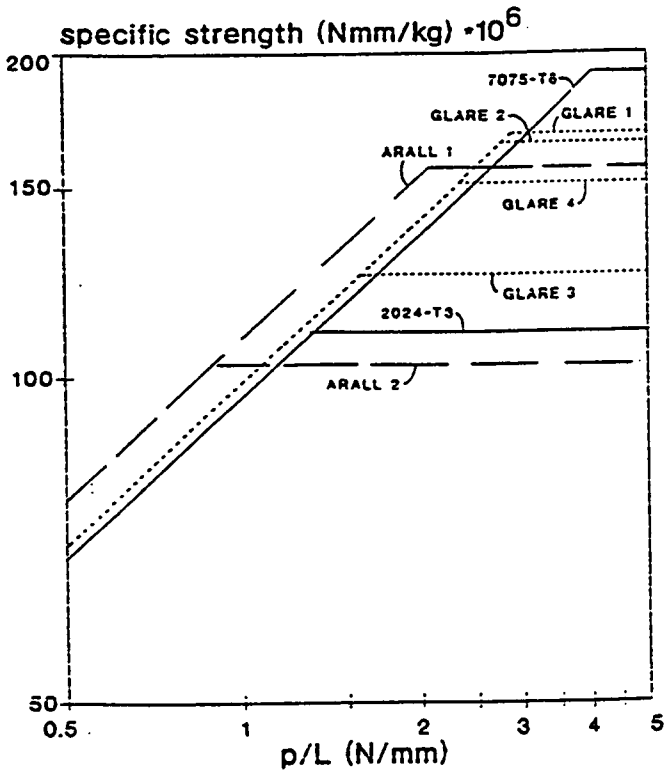

Figure 4.3A : Specific compressive strength as a function of the loading intensity.
PART A : standard GLARE.

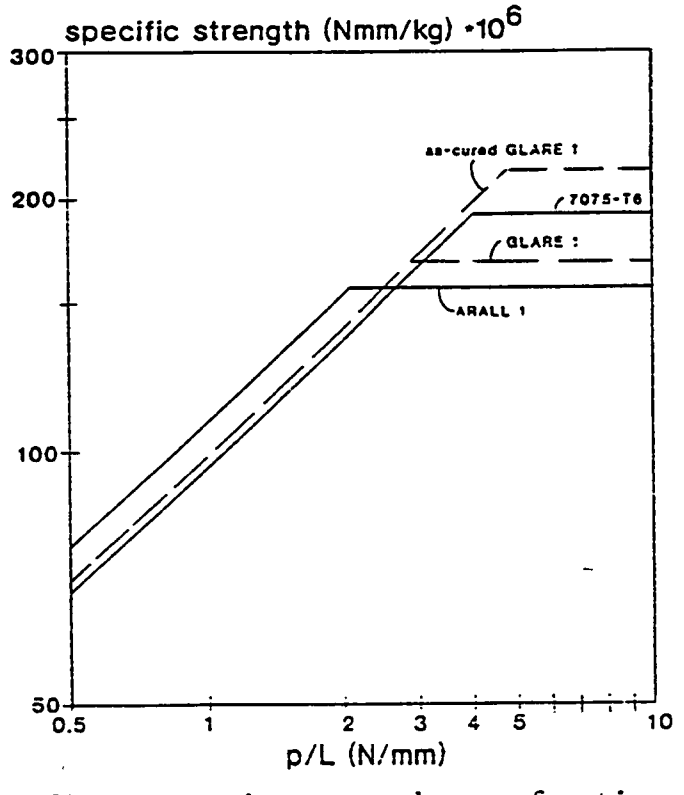

Figure 4.3B : Specific compressive strength as a function of the loading intensity.
PART B : as-cured GLARE 1.

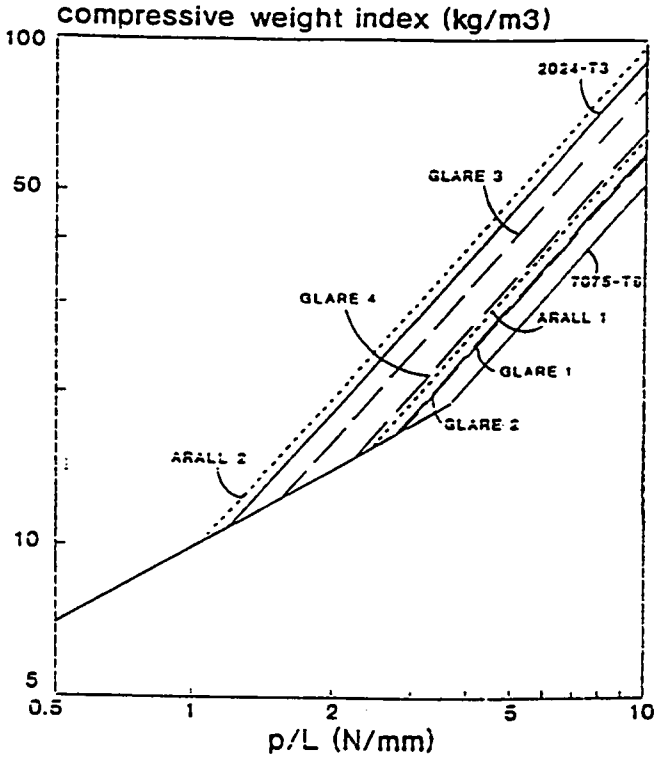

Figure 4.4A : Compressive weight index as a function of the loading intensity.
PART A : standard GLARE.

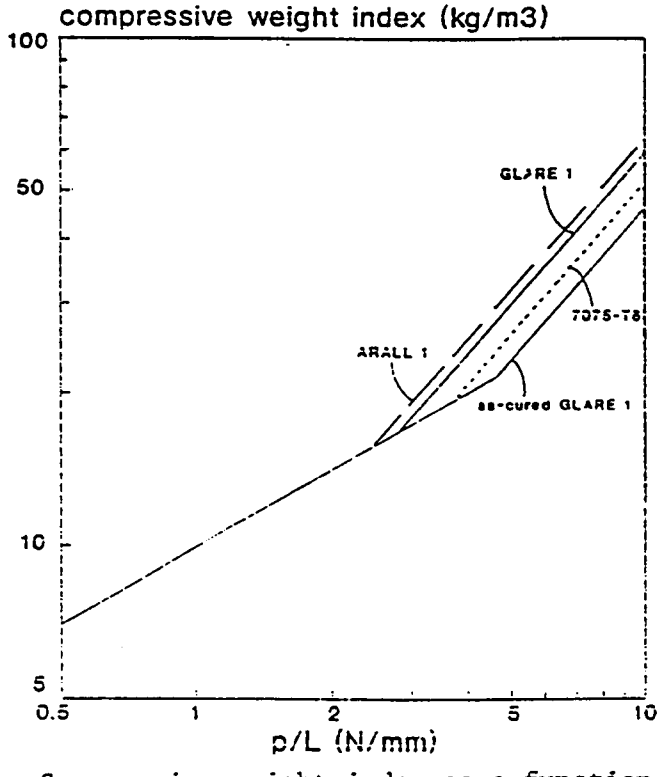

Figure 4.4B : Compressive weight index as a function of the loading intensity.
PART B : as-cured GLARE 1.

Chapter 5 : Prediction methods for Young's modulus and yield stress

§ 5.1 : Young's modulus

Young's modulus is predicted by the rule of mixtures. Because post-stretching has no influence on Young's modulus no calculations were done for as-cured GLARE 1.

The rule of mixtures method basically is the addition of the Young's moduli of the constituents taking into account the thicknesses of the separate layers:

$$E_{tot} = E_{pr} \cdot \frac{\Sigma t_{pr}}{\Sigma t_{pr} + \Sigma t_{al}} + E_{al} \cdot \frac{\Sigma t_{al}}{\Sigma t_{pr} + \Sigma t_{al}}$$

with
E_{pr} = Young's modulus of the prepreg
E_{al} = Young's modulus of the aluminium
} *Table 4.3*

Σt_{pr} = total thickness of all prepreg layers
Σt_{al} = total thickness of all aluminium layers.

The values obtained by this method are listed in *Table 5.1.*

grade	lay-up	dir.	E_{exp} (GPa)	E_{theor} (GPa)	error (%)
GLARE 1	2/1	L	67.7	68.0	0.4
		LT	56.2	56.0	-0.4
GLARE 1	3/2	L	66.5	66.4	-0.2
		LT	51.1	51.3	0.4
GLARE 1	4/3	L	62.4	65.4	2.1
		LT	47.3	48.1	1.7
GLARE 2	2/1	L	69.2	69.5	0.4
		LT	56.4	57.9	2.6
GLARE 2	3/2	L	68.3	68.4	0.1
		LT	53.2	54.6	2.6
GLARE 2	4/3	L	67.4	67.4	--
		LT	51.2	52.0	1.5
GLARE 3	2/1	L	62.8	64.4	2.5
		LT	61.8	64.4	4.0
GLARE 3	3/2	L	59.5	61.0	2.5
		LT	59.7	61.0	2.1
GLARE 4	2/1	L	62.0	62.1	0.2
		LT	56.5	57.3	1.4
GLARE 4	3/2	L	60.8	59.7	1.8
		LT	54.4	53.9	-0.9

Remark : dir. means direction.

Table 5.1 : Comparison between the experimental and the through the rule of mixtures calculated Young's moduli for GLARE.

Also included in this table are the experimental values for GLARE (from *Table 4.1*). As can be seen the accuracy of the rule of mixtures method is excellent.

§ 5.2 : Yield stress

For the prediction of the yield stress the residual internal stress system has to be known. These residual internal stresses in the aluminium and prepreg layers are caused during the curing process, due to the difference in thermal expansion coefficients.
The residual stress in the aluminium layers is[5.1]

$$\sigma_{1,al} = \sigma_{1,al_T} + \sigma_{1,al_{pl}}$$

where the stress in the aluminium due to curing is

$$\sigma_{1,al_T} = E_{al} \cdot \frac{\Delta\alpha . \Delta T . E_{1,pr} . \Sigma t_{pr}}{E_{1,pr} . \Sigma t_{pr} + E_{al} . \Sigma t_{al}}$$

and due to post-stretching

$$\sigma_{1,al_{pl}} = - \frac{E_{1,pr} \Sigma t_{pr} \epsilon_{1,pl}}{\Sigma t_{al}}$$

with

$$\Delta\alpha = \alpha_{1,pr} - \alpha_{al}$$
$$\Delta T = T_{use} - T_{cure}$$
$$\epsilon_{1.pl} = \text{post-stretch percentage.}$$

The internal stress in the prepreg layer is (force equilibrium):

$$\sigma_{1,pr} = - \frac{\sigma_{1,al} . \Sigma t_{al}}{\Sigma t_{pr}}$$

In *Table 5.2* the properties of the prepreg and the aluminium are listed.
In *Table 5.3* the results for post-stretched GLARE 1 and standard GLARE are listed, while in *Table 5.4* the as-cured GLARE 1 values can be found.

	E_1 (GPa)	E_2 (GPa)	α_1 1/K	α_2 1/K
UD prepreg	53.1	11.2	$6.15\ 10^{-6}$	$2.62\ 10^{-5}$
50/50 cross-ply pr.	33.4	33.4	$99.8\ 10^{-7}$	$99.8\ 10^{-7}$
70/30 cross-ply pr.	38.7	25.4	$8.49\ 10^{-6}$	$12.3\ 10^{-6}$
aluminium 7075-T6	74.0	74.0	$23.4\ 10^{-6}$	$23.4\ 10^{-6}$
aluminium 2024-T3	75.8	75.8	$23.4\ 10^{-6}$	$23.4\ 10^{-6}$

Remark: pr. means prepreg.

Table 5.2 : Properties of R-glass prepreg and aluminium[5.2].

grade	lay-up	dir.	σ_1 (MPa)	σ_2 (MPa)
as-cured *GLARE 1*	2/1	L	-69.8	33.7
		LT	2.7	-1.3
as-cured *GLARE 1*	3/2	L	-64.3	40.7
		LT	2.7	-1.7
as-cured *GLARE 1*	4/3	L	-61.8	43.8
		LT	2.7	-1.9

Remark : σ_1 is the internal stress in the prepreg layer(s) and σ_2 in the aluminium layers.

Table 5.4 : Internal stresses for as-cured GLARE 1.

grade	lay-up	dir.	σ_1 (MPa)	σ_2 (MPa)
post-st *GLARE 1*	2/1	L	205.8	-82.3
		LT	2.8	-1.1
post-st *GLARE 1*	3/2	L	212.5	-120.4
		LT	2.7	-1.5
post-st *GLARE 1*	4/3	L	217.0	-151.9
		LT	2.7	-1.9
GLARE 2	2/1	L	-74.2	28.5
		LT	2.8	-1.1
GLARE 2	3/2	L	-69.8	34.1
		LT	2.7	-1.3
GLARE 2	4/3	L	-66.3	38.7
		LT	2.7	-1.6
GLARE 3	2/1	L	-38.4	14.1
		LT	-38.4	14.1
GLARE 3	3/2	L	-36.0	19.2
		LT	-36.0	19.2
GLARE 4	2/1	L	-46.0	26.8
		LT	-23.7	13.8
GLARE 4	3/2	L	-42.6	32.7
		LT	-22.5	17.2

Remarks :- σ_1 is the internal stress in the prepreg layer(s) and σ_2 in the aluminium layers.

- post-st means post-stretched.

Table 5.3 : Internal stresses for GLARE.

The theoretical method to determine the yield stress is based on the stress-strain curves of the constituents (*Figure 5.1*).
The calculation sequence is:

1) $\Delta\sigma = \sigma_{0.2,al} - \sigma_2$

with σ_2 = internal stress in aluminium layers.

2) $\Delta\epsilon = \frac{\Delta\sigma}{E_{al}} - 0.002$

3) $\Delta\sigma_{pr} = E_{pr} \cdot \Delta\epsilon$

4) $\sigma_{pr,tot} = \Delta\sigma_{pr} + \sigma_1$

with σ_1 = internal stress in prepreg layers.

5) $\sigma_{0.2,tot} = \frac{\sigma_{pr,tot} \cdot \Sigma t_{pr} + \sigma_{0.2,al} \cdot \Sigma t_{al}}{\Sigma t_{pr} + \Sigma t_{al}}$

In *Table 5.5* to *5.6* the obtained values can be compared with the experimental ones. The prediction method for the yield stress is, despite its simplicity, pretty accurate (90 %).

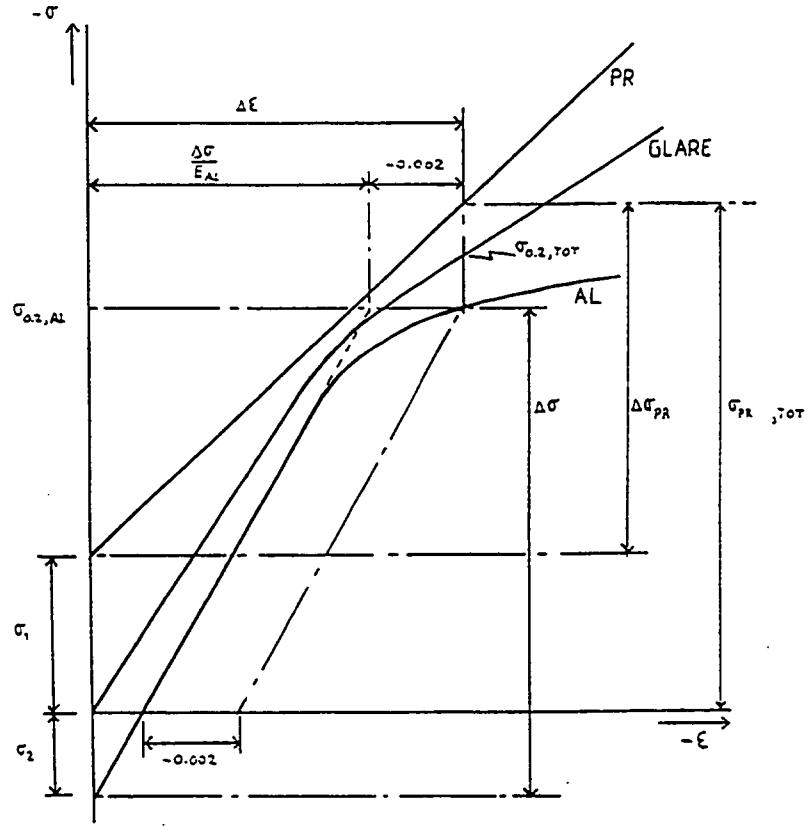

Figure 5.1 : Prediction of the yield stress.

grade	lay-up	dir.	$\sigma_{0.2_{exp}}$ (MPa)	$\sigma_{0.2_{th.}}$ (MPa)	error (%)
as-cured *GLARE 1*	2/1	L	546.4	549.3	0.5
		LT	400.1	399.1	-0.2
as-cured *GLARE 1*	3/2	L	564.9	552.1	-2.3
		LT	375.6	371.7	-1.0
as-cured *GLARE 1*	4/3	L	576.6	553.4	-4.0
		LT	344.5	359.8	4.3

Table 5.6 : Theoretical compressive yield stress for as-cured GLARE 1

grade	lay-up	dir.	$\sigma_{0.2_{exp}}$ (MPa)	$\sigma_{0.2_{th.}}$ (MPa)	error (%)
post-st *GLARE 1*	2/1	L	446.5	444.8	-0.4
		LT	427.0	417.3	-2.3
post-st *GLARE 1*	3/2	L	423.7	408.9	-3.5
		LT	402.7	383.9	-4.7
post-st *GLARE 1*	4/3	L	406.5	380.6	-6.4
		LT	374.5	361.9	-3.4
GLARE 2	2/1	L	389.5	337.0	-13.5
		LT	252.5	270.8	6.8
GLARE 2	3/2	L	420.0	342.4	-18.5
		LT	241.0	256.7	6.1
GLARE 2	4/3	L	421.7	346.6	-17.8
		LT	232.2	245.6	5.5
GLARE 3	2/1	L	319.3	299.6	-6.2
		LT	318.2	334.9	5.0
GLARE 3	3/2	L	314.4	297.5	-5.4
		LT	316.4	331.2	4.5
GLARE 4	2/1	L	349.0	302.0	-13.4
		LT	299.2	291.5	-2.6
GLARE 4	3/2	L	370.9	331.0	-10.8
		LT	291.5	281.5	-3.4

Table 5.5 : Theoretical compressive yield stress for standard GLARE.

Chapter 6 : Conclusions

GLARE laminates in compression are superior to aluminium and certainly to ARALL laminates.
From structural efficiency plots it can be deduced that GLARE is far preferred to ARALL or aluminium for compressive critical structures.
The rule of mixtures method to determine Young's modulus is very simple as well as accurate.
The yield stress can be predicted with an accuracy higher than about 90 %, which is also a good prediction.
From structural efficiency plots it turns out that in buckling dominated structures, ARALL is the best material and GLARE second best, where in the compressive strength dominated structures, GLARE is far superior to ARALL and aluminium and aluminium even better than ARALL.
It must be kept in mind that as cut-off values the yield stress was taken. However this report shows an enormous increase in compressive strength over the yield strength for GLARE which improve the compressive strength dominated structures in GLARE even further.

Literature

1.1 Vogelesang, L.B. and Gunnink, J.W., "ARALL: a materials challenge for the next generation of aircraft", Materials & Design, Vol.7, November 1986

1.2 Gunnink, J.W., "Design studies of primary aircraft structures in ARALL laminates", Journal of Aircraft, Vol.25, November 1988

1.3 Verbruggen, M.L.C.E., "ARALL adhesion problems and environmental effects", Report LR-504 and LR-505, Faculty of Aerospace Engineering, Delft University of Technology, November 1986

1.4 Vermeeren, C.A.J.R., et al., "New developments in fibre metal laminates (ARALL)", Proceedings international symposium ESA, ESTEC, Noordwijk, March 1990

1.5 Vogelesang, L.B. and Roebroeks, G.H.J.J., "Fatigue of fibre metal laminates", 7th international spring meeting, Fatigue of MMC and multimaterial, Paris, June 1990

1.6 Vlot, A., "Impact tests on aluminium 2024-T3, aramid and glass reinforced aluminium laminates and thermoplastic composites", Report LR-534, Faculty of Aerospace Engineering, Delft University of Technology, October 1987

5.1 Eikelboom, M.F., "Theoretisch en experimenteel onderzoek naar het statisch gedrag van gekerfd en ongekerfd ARALL materiaal", MS-thesis (in Dutch), Department of Aerospace Engineering, Delft University of Technology, August 1981

5.2 Verolme, J.L., "The compressive properties of GLARE", TZ report, Department of Aerospace engineering, Delft University of Technology, November 1990

A.1 Anon., "Buckling of rectangular specially orthotropic plates", Engineering Science Data Unit (ESDU) Item number 80023

A.2 Jones, R.M., "Mechanics of composite materials", Institute of Technology, Southern Methodist University, Dallas, Texas, McGraw-Hill book company, 1975 (ISBN 0-07-032790-4)

A.3 Gunnink, J.W. and v.d.Schee, P.A., "Design of the ARALL F-27 lower wing fatigue panel", 4th intern. conference on composite structures, Paisley, Scotland, July 1987

A.4 Rothwell, A., "An experimental investigation of the efficiency of a range of channel section struts", Aeronautical Journal, 1974

A.5 Slagter, W.J., "Assesment of coefficients of thermal expansion for UD-FRC", Memorandum M-597, Department of Aerospace Engineering, Delft University of Technology, July 1988

Appendix : Details on the construction of structural efficiency plots.

The two demands dictating the stress level in compressive critical stringer-skin panels are (in this report):

1 No Euler buckling

2 The yield stress is the cut-off value.

These two demands can be written as a function of the structural index:

1 No Euler buckling

For overall buckling Euler's formula may be used, in the form

$$\sigma_f = C_1 . E_x . \left(\frac{b}{L_e} \right)^2$$

with $C_1 = \frac{\pi^2 . I}{b^2 . A}$

I = moment of inertia of cross-section relatively to the neutral axis

E_x = longitudinal Young's modulus of the laminate.

We may also define an equivalent thickness (the thickness of a same plate containing the same quantity of material)

$$\bar{t} = C_2 . t$$

The loading p is defined as

$$p = \sigma . \bar{t}$$

Putting for an efficient design

$$\sigma = \beta . \sigma_1 = \sigma_f$$

where σ_1 is the local buckling stress.

For the local buckling stress of a long, all edges simply-supported, specially orthotropic† plate applies[A.1]

$$\sigma_1 = \frac{2\pi^2}{b^2 t} \cdot \left(\sqrt{D_{11} D_{22}} + D_{12} + 2.D_{66} \right)$$

with b = width of plate

t = thickness of plate.

In this formula the factors D_{ij} are the bending stiffnesses defined in the classical lamination theory. The calculation procedure for these factors can be found in *Literature A.2*. The equation can be rewritten as

$$\sigma_1 = \frac{2\pi^2}{b^2 t} \cdot \left(\frac{D^* . t^3}{6} \right)$$

$$\text{with} \quad D^* = \frac{6}{t^3} \left(\sqrt{D_{11} D_{22}} + D_{12} + 2.D_{66} \right)$$

Combining all above mentioned formulas and eliminating the dimensions b and t leads to

$$\frac{\sigma}{\rho} = \left(\frac{2\pi^2}{6} \right)^{1/4} \cdot \left(\frac{C_1}{C_2^2} \right)^{1/4} \cdot \beta^{1/4} \cdot \left(E_x . D^* \right)^{1/4} \cdot \sqrt{\frac{p}{L_e}}$$

For the compressive weight index can be written:

$$\frac{W}{A.L_e} = \frac{\rho . b . \bar{t} . L}{b . L . L_e} = \frac{\rho . \bar{t}}{L_e} = \rho . \frac{1}{\sigma} . \frac{p}{L_e}$$

so

$$\frac{W}{A.L_e} = \rho . \left(\frac{6}{2\pi^2} \right)^{1/4} \cdot \left(\frac{C_2^2}{C_1} \right)^{1/4} \cdot \left(\frac{1}{\beta} \right)^{1/4} \cdot \left(\frac{1}{E_x . D^*} \right)^{1/4} \cdot \sqrt{\frac{p}{L_e}}$$

†Specially orthotropic means that the material axes are aligned with the natural body axes of the laminate.

2 No stress higher than the yield stress

This requirement simply leads to

$$\frac{\sigma}{\rho} = \frac{\sigma_{0.2}}{\rho} \qquad \text{and} \qquad \frac{W}{A.L_e} = \frac{\rho}{\sigma_{0.2}} \cdot \frac{p}{L_e}$$

Determination of the constants

The structural efficiency plots are valid for a specific stringer-skin panel, and are merely meant for comparative reasons.

In this report the stringer-skin panel is the lower skin of the outerwing of the Fokker F-27. In *Figure A.1* the shape of this panel is given (taken from *Literature A.3*). The Z-stringer in detail A is chosen.

A diagrammatic picture of this stringer is shown in *Figure A.2*.

So the dimensions of the stringer (and the stringer pitch) are:

$b_1 = 42$ mm $h = 38$ mm

$b_2 = 28$ mm $t_1 = 1.8$ mm

$b_3 = 25$ mm $t_2 = 1.3$ mm

$b_4 = 10$ mm

The neutral axis is located at a distance y from the skin:

$$y.A_{tot} \cong \tfrac{1}{2}b_1t_1^2 + \tfrac{1}{2}b_2t_1^2 + b_2t_2(t_1 + \tfrac{1}{2}t_2) + ht_2(t_1 + \tfrac{1}{2}h) + \\ + b_3t_2(t_1 + h - \tfrac{1}{2}t_2) + b_4t_2(t_1 + h - \tfrac{1}{2}b_4)$$

with $A_{tot} = t_1(b_1 + b_2) + t_2(b_2 + h + b_3 + b_4)$

and the above mentioned dimensions follows:

$A_{tot} = 257.3$ mm^2 ; $y = 11.48$ mm

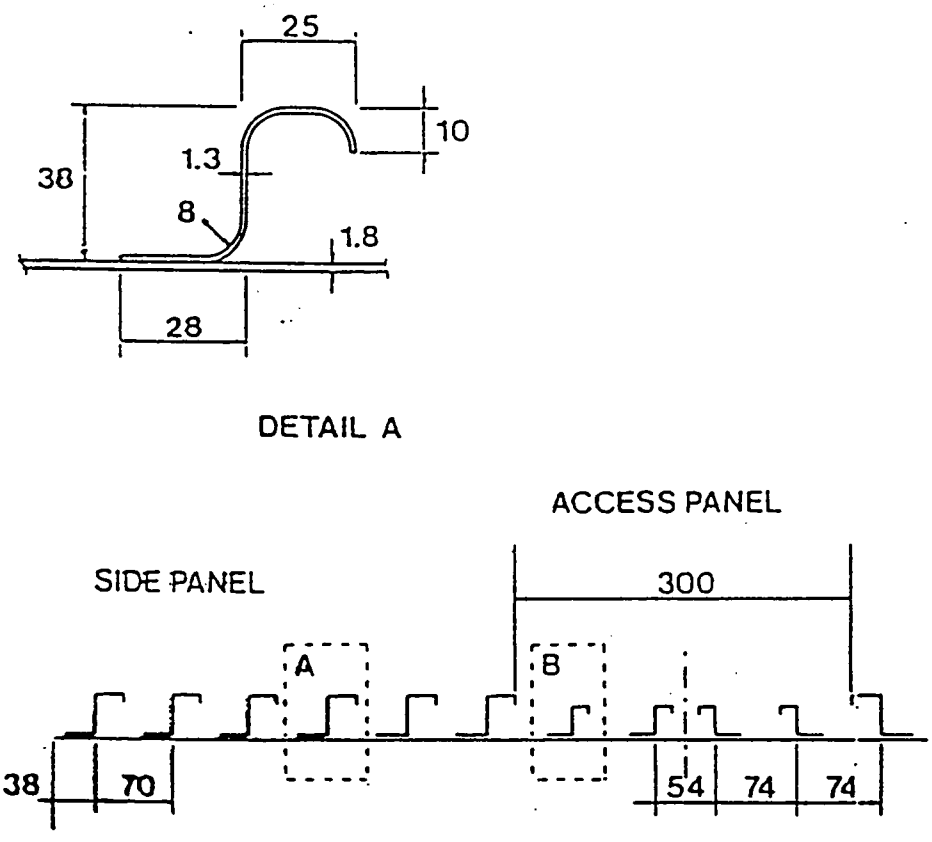

Figure A1 : The lowerskin panel of the outerwing of the Fokker F-27

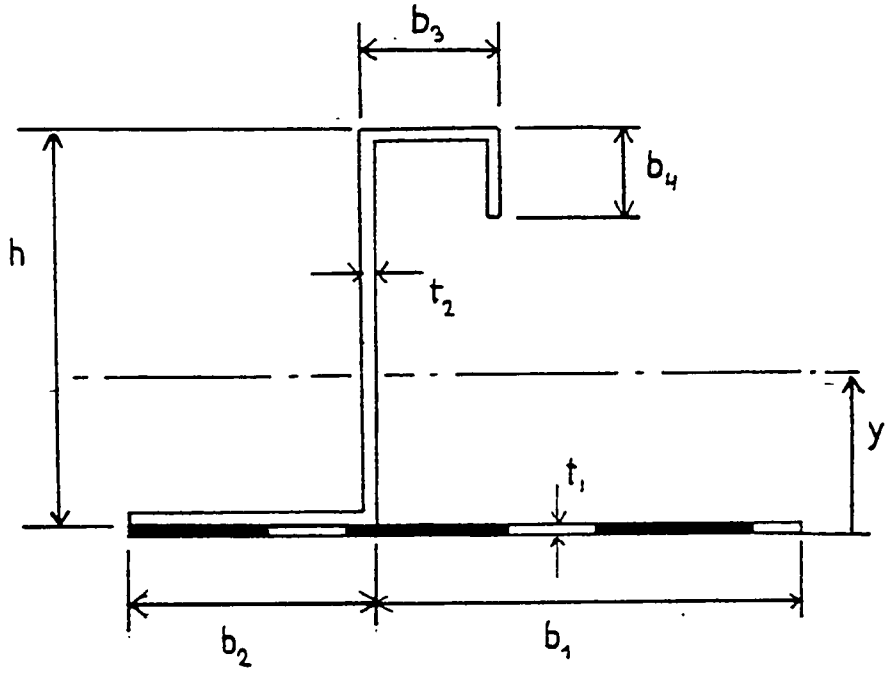

Figure A2 : Diagrammatic picture of the Z-stringer

The moment of inertia relatively to the neutral axis can be calculated:

$$I \cong \frac{1}{12}b_1t_1^3 + b_1t_1y^2 + \frac{1}{12}b_2t_1^3 + b_2t_1y^2 + \frac{1}{12}b_2t_2^3 + b_2t_2y^2 +$$
$$+ \frac{1}{12}t_2h^3 + ht_2(\frac{1}{2}h - y)^2 + \frac{1}{12}b_3t_2^3 + b_3t_2(h - y)^2 +$$
$$+ \frac{1}{12}t_2b_4^3 + t_2b_4(h - \frac{1}{2}b_4 - y)^2 = 59171 \text{ mm}^4$$

So

$$C_1 = \frac{\pi^2.I}{b_1^2.A_{tot}} = \frac{\pi^2.59171}{(42)^2.257.3} = 1.287$$

$$C_2 = \frac{A_{tot}}{(b_1 + b_1)t_1} = \frac{257.3}{(42+28).(1.8)} = 2.042$$

This leads to $\left(\frac{C_1}{C_2^2}\right)^{1/4} = 0.7454$

and $\left(\frac{C_2^2}{C_1}\right)^{1/4} = 1.3416$

An optimum value for the factor β seems to be β=0.8 (see *Literature A.4*). This means that the overall buckling stress is slightly lower than the local buckling stress. Two main advantages are the insensitivity to imperfections of the panel and the absence of interaction between local and overall buckling (because of local buckling there is a loss of compressive stiffness which reduces the overall buckling stress).

For aluminium (isotropic material) $E_x.D^*$ reduces to

$$E_x.D^* = \frac{E^2}{1-\mu^2}$$

The values for the yield stress, density and Young's modulus used to construct the curves can be found in *Table A.1*.

type	E_c (GPa)	density (g/cm^3)	$\sigma_{0.2,c}$ (MPa)
2024-T3	75.8	2.78	306.9
7075-T6	74.0	2.78	533.1
GLARE 1	66.5	2.52	423.7
as-cured *GLARE 1*	66.5	2.52	564.9
GLARE 2	68.3	2.52	420.0
GLARE 3	59.5	2.52	314.4
GLARE 4	60.8	2.45	370.9
ARALL 1	70.0	2.33	365.0
ARALL 2	67.0	2.33	240.0

Table A.1 : The values of Young's modulus, density and yield stress used in the structural efficiency plots.

The figures are constructed for 3/2 lay-ups of ARALL as well as GLARE. The properties of the aramid and R-glass prepregs are listed in *table A.2*. These properties are needed to calculate the bending stiffnesses of the laminates.

	aramid prepreg	R-glass prepreg
E_1 (MPa)	63000	53100
E_2 (MPa)	4000	11200
μ_{12}	0.345	0.33
G (MPa)	1236	6074
t (mm)	0.2	0.125

Table A.2 : Properties of aramid[A.5] and R-glass prepregs.